Electron rich substituted β-carboline derivatives: Synthesis and photophysical properties

Corentin Maret, Sarah Chebourou, Antoinette de Nicola, Thomas Papineau, Morgane Vacher, Denis Jacquemin, Gilles Ulrich

Electron rich substituted β-carboline derivatives: synthesis and photophysical properties

Corentin Maret,[a] Sarah Chebourou,[a] Antoinette De Nicola,[a] Thomas V. Papineau,[b] Morgane Vacher,[b] Denis Jacquemin*[b,c] and Gilles Ulrich*[a]

a) Institut de Chimie et procédés pour l'Energie, l'Environnement et la Santé (ICPEES), Groupe de Chimie Organique pour les Matériaux, la Biologie et l'Optique (COMBO), CNRS UMR 7515, École de Chimie, Polymères, Matériaux de Strasbourg (ECPM), 25, Rue Becquerel, 67087 Strasbourg, Cedex 02, France
b) Nantes Université, CNRS, CEISAM, UMR 6230, 44000 Nantes, France. E-mail: Denis.Jacquemin@univ-nantes.fr
c) Institut Universitaire de France (IUF), 75005 Paris, France

Abstract :

We report the synthesis and characterisation of known and novel analogues of β-carboline, a naturally occurring alkaloid. Striving to induce changes in the optical properties of carboline, we first focus on substitutions at position 1 before exploring other positions. The β-carbolines were synthesized using, on the one hand, post-synthetic functionalization of biosourced products and, on the other hand, total synthesis of the desired compounds. Our strategy mainly relies on the well-known Pictet-Spengler reaction, followed by aromatization using different techniques. Post functionalization were performed by Knoevenagel condensation or pallado-catalyzed cross-coupling. The measured UV-visible and fluorescence spectra show unexpected results with large shifts obtained when changing a few substituents only. For instance, the replacement of the aryl by a styryl substituent induces a bathochromic shift as large as 70 nm. This allowed controlling the position of the emission on a broad range (from 370 and 650 nm). Additionally, protonation of the compounds leads to profound changes in the spectroscopic properties. We indeed observe for some compounds a bathochromic shift in the emission as large as 200 nm upon protonation. The main experimental results are rationalized using theoretical calculations.

Keywords: β-carboline, Photoluminescence, TD-DFT calculations

Introduction

Indole alkaloids are the most widespread family of alkaloids, with more than a third of them derived from this skeleton.[1] β-carbolines belong to this group with a structure resulting from the fusion of a six membered ring containing a nitrogen on the second position and an indole ring. There are different degrees of saturation on the pyridinic ring, allowing access to diverse β-carbolines from the fully insaturated ones to their dihydro and tetrahydro counterparts. This skeleton is widely distributed in nature as a secondary metabolite of the plant kingdom.[2] Their use is ancestral, Amazonian tribes using a β-carboline derivative as a hallucinogenic infusion for more than 3000 years.[3] Another application is *Peganum Harmala* seeds, which contain a high concentration of harmine, harmaline, and harmol and has been used in the treatment of diabetes or hypertension.[4] Indeed, both synthetic and natural β-carbolines show a wide range of biological properties with, *e.g.*, interaction with benzodiazepine receptors, [5] intercalation in DNA,[6] inhibition of monoamino oxidase,[7] etc. In addition, the skeleton is known for its numerous pharmaceutical properties.[8] The majority of previous investigations logically focussed on synthetic aspects as well as on the evaluation of the biological responses of the obtained derivatives. For example, tadalafil,[9] cipargamine[10] and abecarnil[11] are three drugs that contain the β-carboline skeleton (Scheme 1).

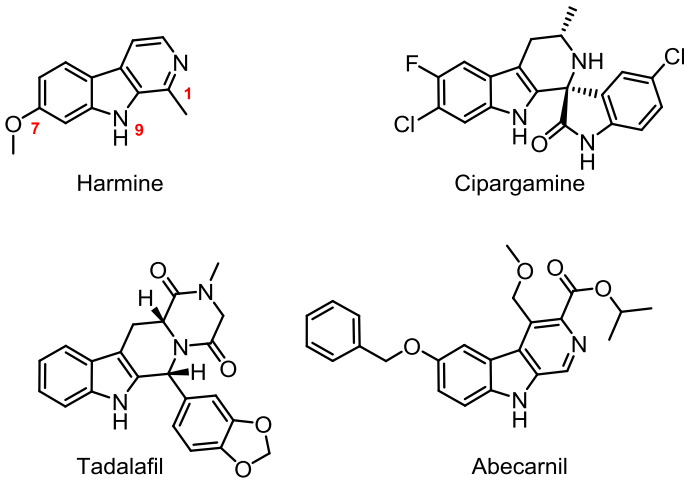

Scheme 1 Different β-carboline derivates possessing bioactive properties

Beside their biological properties, β-carbolines exhibit intense blue fluorescence. It is notably observed in scorpion cuticles, giving them their hallmark bright blue colour under UV light,[12] although some authors suggested that this blue emission might originate from coumarin derivatives.[13-14] An interesting feature of carboline fluorescence is the possible simultaneous presence of several acid-base forms. Indeed, depending on the pH, the pyridine nitrogen is protonated or the indole nitrogen is deprotonated.[15] We also underline that β-carboline possesses resonance structures that may arise under polar and protic conditions, leading to a quinoid form of the molecule. This is due to a hydrogen bonding complex that forms between the two nitrogen sites, producing a redshifted intramolecular charge-transfer (ICT) emission.[16-17] Carbolines have also been used as solid emitters,[18] water detectors[19] or optical sensors for copper and fluorine.[20]

From this analysis, it turns out that the photophysical properties of β-carboline derivatives remain mostly under investigated. In fact, only the simplest alkaloids of β-carboline such as harmane, harmine, harmol, and some closely-related derivatives have been studied for their photophysical properties.[15] Reports on the photophysical properties of more substituted β-carbolines are rather scarce in the literature.[15–17,21–30] Given the lack of studies of β-carboline absorption and fluorescence, we propose in the present work to explore the impact of the substitution at position 1 on the spectral properties of neutral and protonated β-carboline derivatives. In more details, the substitution by two electron donating groups (methoxy and dimethylamino), one accepting moiety (trifluoromethyl), connected through three different spacers (aryl, styryl and ethynyl) are investigated.

Synthesis

To synthesize the 1-aryl-β-carbolines **2a-c** we selected the Pictet-Spengler reaction[21] starting from tryptophan **1** and substituted benzaldehyde under acidic conditions. The intermediate tetrahydro-β-carboline was used without further purification (Scheme 2) and treated with the NCS/TEA couple followed by addition of hydrogen peroxide to promote a decarboxylation/aromatisation reaction to obtain the compounds **2a-c** with an overall yield between 15 and 43%.

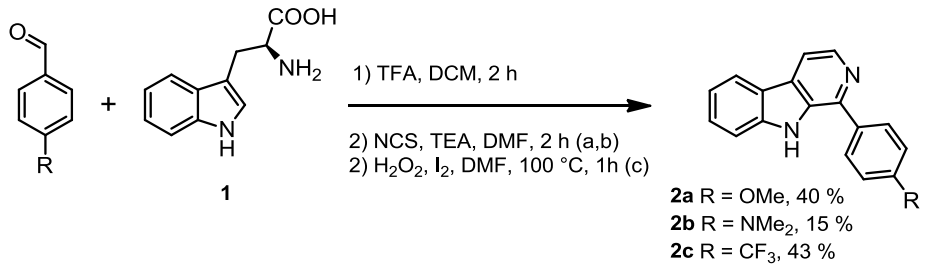

Scheme 2 Synthesis of 1-aryl-β-carbolines

To introduce a double bound spacer between the functional aryl group and the carboline, we started from natural occurring β-carboline harmane **3** and harmine **3'** (Scheme 3). Compound **3'** was used as received from commercial sources and **3** was synthesized using the same reaction as for **2** with a yield of 36 % over two steps, using acetaldehyde (Scheme 3).[31] Compounds **3** and **3'** were then reacted in a Knoevenagel condensation in the presence of piperidine and *p*-toluenesulfonic acid to form the corresponding 1-styryl-β-carbolines **4a-b** and **4'b** with various yields. The alkenes were more problematic to purify likely due to easy isomerization of the double bond under light and chromatography condition. The products **4a-b** and **4'b** were obtained pure after multiple recrystallizations.

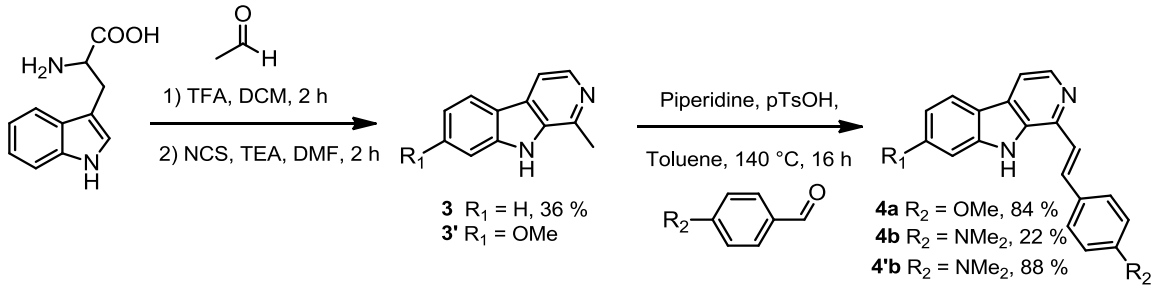

Scheme 3 Synthesis of 1-aryl-β-carbolines

The 1-bromo-β-carboline **5** was prepared according to literature report [32] and obtained with a yield of 59 % from 1-hydroxy-β-carboline (Scheme 4). The bromo derivative **5** was then reacted with various alkynes under Sonogashira cross coupling condition to yield 1-ethynyl-β-carbolines **6a-b** with good yields (Scheme 4).

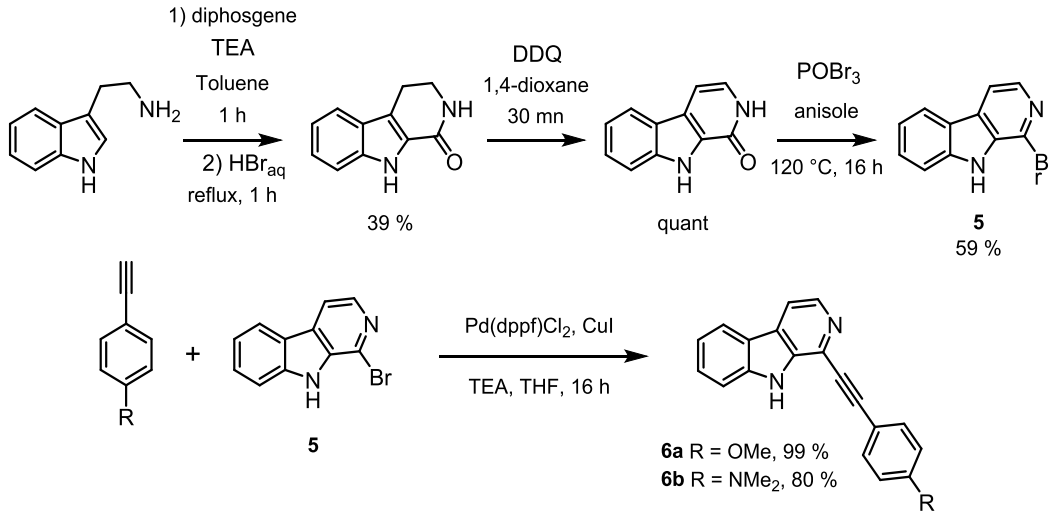

Scheme 4 Synthesis of 1-aryl-β-carbolines

Spectroscopic properties

The electronic absorption and emission spectra of the chromophores **2a**, **2b**, **2c 4a**, **4b, 4'b**, **6a**, and **6b** were recorded in solvent of various dielectric constant and proticity. Solution in ethanol were recorded with and without the addition of HCl_g. All the data can be found in Table I.

	λ_{abs} (1) (nm)	ε (2) ($M^{-1}.cm^{-1}$)	λ_{em} (3) (nm)	Φ_f (4) (%)	Δ^{ss} (5) (cm^{-1})	τ (6) (ns)	k_r (7) (10^8 s^{-1})	k_{nr} (7) (10^8 s^{-1})	Solvent
2a	354	7300	374	21	1510	5.51	0.38	1.43	Benzene
	354	7700	374	23	1510	5.81	0.39	1.33	DCM
	359	6900	381	22	1608	1.74	1.26	4.48	EtOH
	386	7100	445	6	3435	15.1	0.04	0.62	EtOH + HCl
2b	359	16100	413	52	3642	2.43	2.14	1.98	Benzene
	362	16200	430	61	4368	3.38	1.80	1.15	DCM
	365	15600	442	48	4772	2.74	1.75	1.90	EtOH
	418	21600	525	15	4875	14.19	0.11	0.60	EtOH + HCl
2c	355	10100	384	28	2262	1.25	2.24	5.76	Benzene
	354	9000	389	22	2541	1.48	1.49	5.27	DCM
	362	8800	402	26	2748	3.09	0.84	2.39	EtOH
	387	6500	481	13	5049	6.79	0.19	1.29	EtOH + HCl
4a	376	17300	405	38	1905	1.27	2.99	4.88	Benzene
	377	22300	408	12	2015	3.40	0.35	2.59	DCM
	382	20500	413	31	1964	1.64	1.89	4.21	EtOH
	423	16800	nr						EtOH + HCl
4b	396	20500	451	6	3079	3.84	0.16	2.45	Benzene
	394	18000	487	5	4846	4.56	0.11	2.08	DCM
	396	16400	506	9	5411	2.88	0.31	3.16	EtOH

	474	8800	623	23	4482	20.68	0.11	0.37	EtOH + HCl
4'b	397	28700	449	6	2917	0.28	2.14	3.36	Benzene
	395	22400	479	5	4439	2.94	0.17	3.23	DCM
	397	27100	499	5	5148	4.33	0.12	2.19	EtOH
	473	11500	607	26	4667	11.85	0.22	0.62	EtOH + HCl
6a	386	18200	405	15	1215	1.56	0.96	5.45	Benzene
	370	15300	385	24	1053	1.20	2.00	6.33	DCM
	388	15700	425	5	2244	2.76	0.18	3.44	EtOH
	421	10300	525	1	4705	11.32	0.009	0.87	EtOH + HCl
6b	375	26800	412	80	2394	2.43	3.29	0.82	Benzene
	387	31100	449	85	3568	1.55	5.48	0.97	DCM
	393	32000	471	60	4214	5.03	1.19	0.79	EtOH
	457	36700	nr						EtOH +HCl

Table 1 Optical properties of carbolines (1) Absorption wavelength (2) Molar extinction coefficient (3) Emission wavelength (4) Quinine bisulfate (1.0 N H_2SO_4 Φ_f= 0.55) and fluoresceine (0.1N NaOH Φ_f= 0.90, were used as reference.[36] All Φ_f were corrected with the refractive index of the medium, error ±10%. (5) Stokes Shift (6) Lifetime, error ±0.5 ns. (7) Calculated using the following equations: kr= Φ_f / τ and knr = (1-Φ_f)/ τ , assuming that the emitting state is produced with unit quantum efficiency.

Let us first discuss the differences between the methoxy and dimethylamino substitutions using

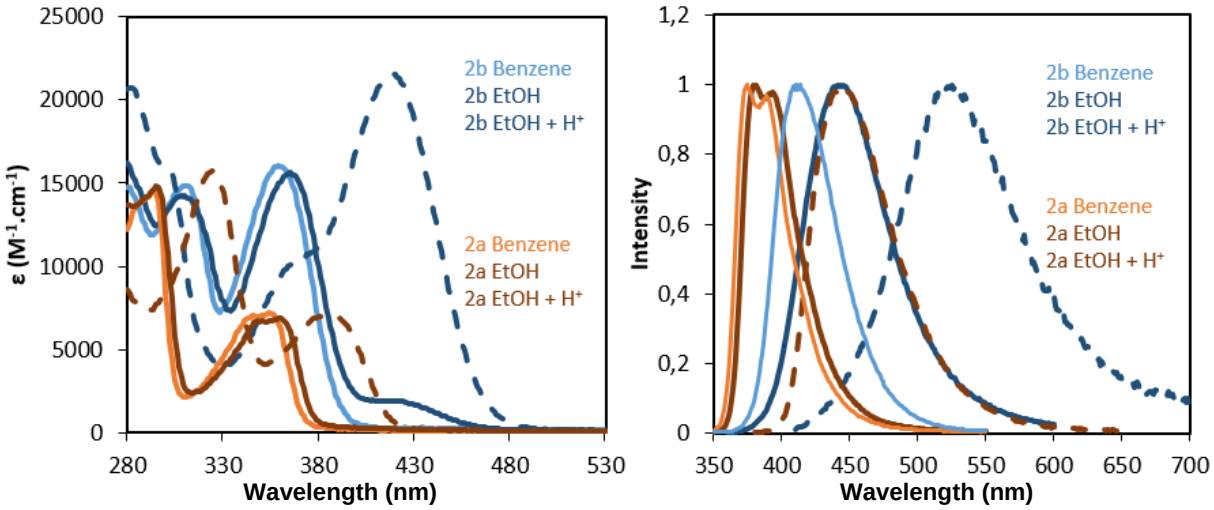

compounds **2a** and **2b**, considering both neutral and protonated dyes. The spectra are given in Figure 1.

Figure 1 Absorption (left) and emission (right) of compounds **2a** and **2b**. The dotted lines correspond to the protonated forms.

For the absorption spectra, the differences between the two electrodonating groups is significant, with a marked hyperchromic displacement when comparing **2b** to **2a**. In ethanol, a small band is also noted at ca. 430 nm for compound **2b**, which is likely due to traces of the protonated compound. For both compounds, bathochromic and hyperchromic shifts are observed upon protonation, an effect which is amplified for **2b**. Measurement in other solvents show little solvatochromic shifts for the neutral form. The fluorescence spectra for compound **2a** exhibit a structured emission in benzene and a Stokes' shift roughly half of the one of **2b,** which can be directly correlated to the smaller variation of dipole moment between ground and excited states in **2a** than in **2b**. The quantum yields measured in ethanol for the neutral compounds are 48% and 22%, respectively for **2b** and **2a**. Upon protonation, large bathochromic shifts of the emission are observed, and the Stokes shift increases up to 4875 cm^{-1} for **2b**, which hints at a significant ICT effect. For practical applications, the most interesting features are the bathochromic shifts observed upon protonation for emission, 3774 cm^{-1} for **2a** and 3576 cm^{-1} for **2b**. There is also a drop in quantum yields upon protonation with 6 % for **2a** and 15 % for **2b**. The lifetimes of the protonated compounds are longer than their neutral counterparts, with a tenfold increase. In the case of compound **2c** (Fig S28-S31), substitution with an electron-withdrawing group shows behaviours close to that of **2a**. The absorption spectra of **2c** show a weak bathochromic shift with increasing solvent polarity. Nevertheless, a clear red shift is observed in the emission spectra compared to **2a**, but not as pronounced as for **2b**. Overall, **2c** shows intermediate properties between **2a** and **2b**, whether in terms of absorption wavelength, emission or its particular behaviour during protonation. From those data, we can conclude that the presence of the dimethylamino group greatly impacts the spectral properties of the 1 substituted β-carboline, as it results in a bathochromic shift of the emission and an increase of both the quantum yield and the molar extinction coefficient. We will now focus only on dimethylamino-substituted β-carboline.

At this stage, we underline that the actual structure of the protonated molecule remains uncertain: is the pyridine moiety, or the amino donor or both groups protonated? Experiments using acetic acid for the protonation showed the same behaviour as protonation with HCl_g indicating that the protonation site is most likely the pyridinic nitrogen. It was also observed that the compounds are partially

protonated in polar solvent, such as ethanol. It suggests that residual water molecules are sufficient to protonate the pyridine ring in dissociative solvents. This experimental analysis is corroborated by theoretical calculations (*vide infra*).

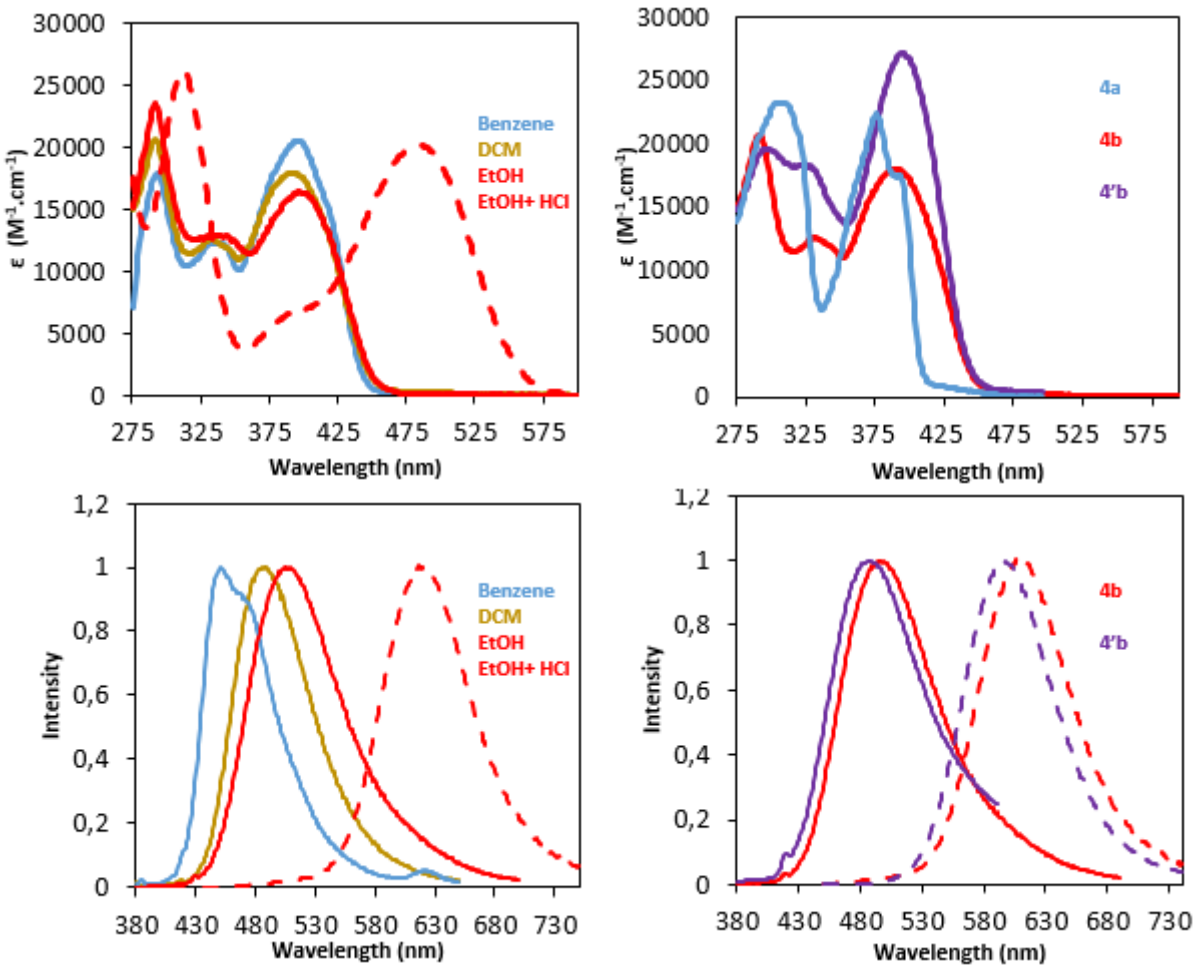

Figure 2 Absorption of **4b** in different solvents (top left); absorption of **4a, 4b**, and **4'b** in ethanol (top right); emission of **4b** in different solvents (bottom left); emission of **4b** and **4'b** in ethanol (plain) and ethanol acidified with HCl_g (dotted) (bottom right).

Figure 2 shows the emission spectra of **4b** in different solvents. In benzene, a solvent with no dipole moment, a structured emission is observed with a typical topology for a S_1-S_0 transition. A small

bathochromic shift is observed as the polarity of the solvent increases with a less structured emission, typical of a shift to emissive ICT state. This observation is common to all the dyes considered herein. As in the **2a**, protonation induces a marked redshift, attributed to the protonation of the pyridyl moiety. The two **4b** molecules are therefore of interest as an emission that practically reaches in the red part of the spectrum can be obtained in acidic ethanol.

Another interesting comparison with this molecule is displayed on the right-hand-side of Figure 2. The comparison of the absorption and emission spectra of **4b** and **4'b** recorded in ethanol indicates that the compound with the methoxy group in the 6 position undergoes a hypsochromic shift in both the neutral and protonated forms. The same behaviour is noted with the solvent change and shows a greater difference in the protonated form.

The difference between the protonated and neutral forms for both compounds may be the mark of a structural change during protonation. The group of Sánchez-Coronilla [16] hypothesized that this could be due to the formation of the quinoid form of the molecule in the protonated state.

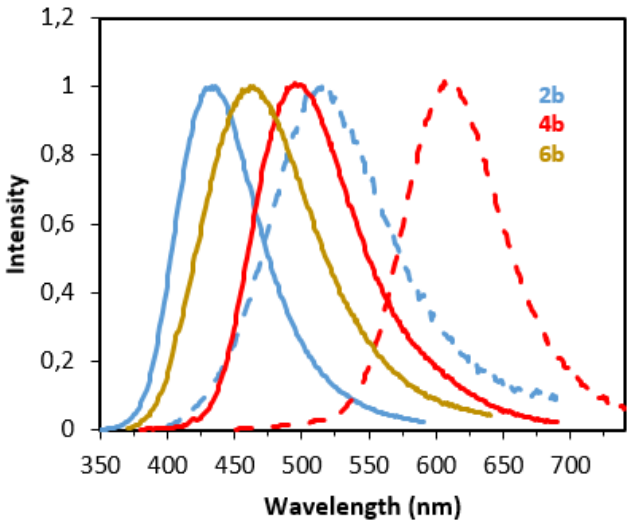

Figure 3 Emission of **2b**, **4b** and **6b** in ethanol (solid) and protonated ethanol (dotted)

The influence of position 1 on the spectral properties has further investigated by comparing the fluorescence spectra of different spacers, all bearing a 4-dimethylamino phenyl moiety (Figure 3). First, their absorption spectra are similar, with a bathochromic shift of ca. 30 nm for **4b** and **6b** as

compared to **2b**. All compounds have in common an unusually large emission band, again indicative of significant ICT. Relatively to their bathochromic shift, the styryl bridge produces the stronger effect, followed by the alkyne and finally the aryl. Upon protonation, compound **6b** becomes non-fluorescent. An interesting effect is noted for **4b**: the quantum yield increases from 9 to 23 % upon protonation, which contrasts with all the other molecules presented here for which the opposite trend is found. The styryl substitution shows interesting features and leads redshifted spectra as compared to all other compounds with emission maxima at 623 nm. It also possesses the largest Stokes' shift recorded for the dyes treated here. Besides that, it's also noted that unlike the other molecules, the absorption spectrum of **4b** undergoes a hypochromic shift upon protonation. This is likely due to the poor solubility of this highly polar molecule in ethanol.

Theoretical modelling

To further characterize the synthesized dyes and rationalize their photophysical behaviour, we use theoretical chemistry. The selected computational protocol, using the Time-Dependent Density Functional Theory (TD-DFT) and second-order Coupled-Cluster (CC2) approaches is described in the SI. The solvent effects are included using the recently-developed cLR^2-PCM model.[33] Let us start by considering the compounds in benzene, an apolar and aprotic solvent for which the applied continuum model likely provides an accurate representation of solvation effects. For all compounds, we found a bright S_0-S_1 transition, with a clear π–π* character. Illustratively, the electron density difference (EDD) plots of **2a-2c** are displayed in Figure 4 (see the SI for other compounds). For **2a**, one notices only a slight contribution from the anisole moiety, and the alternation of density loss/gain, typical of local excited-states. In **2b**, the amino donor plays as expected a significant role and the ICT character from the substituent towards the core is clear. In **2c**, the impact of the trifluoromethyl group is also significant with a reverse ICT, but with a smaller amplitude than in **2b**. As can be seen in Figure S1, when using a styryl linker, the trends noted above pertain, but the transition is more localized on the substituent. One also notices than the additional methoxy group in **4'b** has a very mild role, consistent with the highly similar experimental signatures of **4b** and **4'b**.

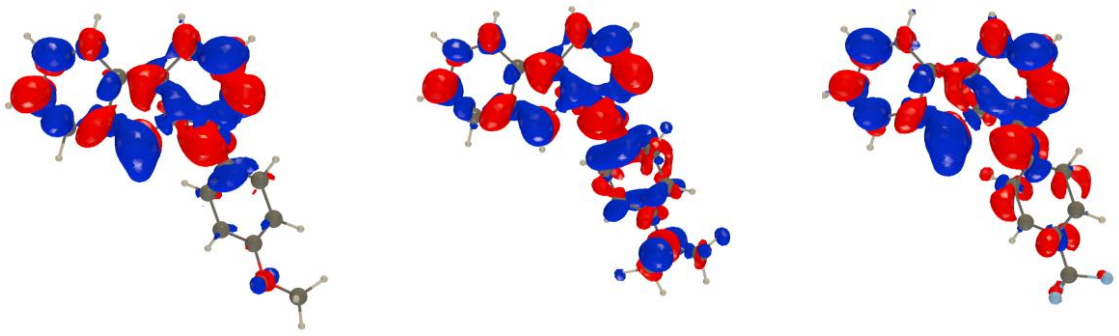

2a **2b** **2c**

Figure 4: EDD plot for the absorption of dyes **2a**, **2b**, and **2c** in benzene. Navy blue and crimson red lobes correspond to decrease and increase of electron density upon photoexcitation, respectively. Contour threshold: 1 x 10^{-3} au.

To have a more quantitative view we have computed the main photophysical parameters for all dyes in benzene, and our results are given in Table 2. First, we note that consistent with the qualitative analysis of the EDD, the ICT parameters as computed with Le Bahers' model,[34] indicate that there is no ICT in **2a**, but a significant one in **2b** (ICT distance of 2.24 Å), and a moderate one in **2c** (1.24 Å). We also note that it clearly appears that the NMe_2 group induces, irrespective of the linker, much more significant ICT than its methoxy counterpart, consistent with the strong solvatochromic effects observed in **2b**, **4b**, **4'b** and **6b** (see Table 1).

Table 2: Main theoretical results obtained in benzene for all dyes using a CC2/TD-DFT/cLR[2] protocol. We report the vertical absorption and emission wavelengths (in nm), the 0-0 energies (in eV) as well as the ICT distance (Å) and charge (e).

	$\lambda^{vert\text{-}abs}$ (nm)	$\lambda^{vert\text{-}fl}$ (nm)	$\Delta E^{0\text{-}0}$ (eV)	d^{CT} (Å)	q^{CT} (e)
2a	327	381	3.40	0.58	0.45
2b	340	404	3.21	2.24	0.55
2c	331	388	3.37	1.24	0.50
4a	362	425	3.01	0.75	0.45
4b	387	458	2.79	2.58	0.53
4'b	384	454	2.81	2.45	0.53
6a	342	381	3.26	0.60	0.47
6b	356	401	3.09	2.59	0.55

In Table 2, we list vertical absorption and fluorescence energies, that have no clear experimental counterparts, but one nevertheless notices that their evolution parallels the positions of the experimental maxima, with, *e.g.*, the two most redshifted emissions for **4b** and **4'b**. Table 2 also reports theoretical 0-0 energies that can be directly compared to the experimental crossing point between the absorption and emission curves.[35] The data of Table 2 yield a rather small mean absolute error (MAE) of 0.09 eV, typical of the used level of theory.[33,35] Another property allowing direct theory-experiment comparisons is the band shape. In Figure S2**,** we report the computed and measured band shapes of the four amino-substituted dyes (**2b**, **4b**, **4'b**, and **6b**), and the good match is obvious.

Looking at the experimental data of Table 1, one clearly notices differences between amino- and methoxy-substituted dyes in terms of both radiative and non-radiative rates, the final quantum yields obtained with the former group being notably larger. To understand the relatively poor photophysical performance of the OMe-dyes, we have performed a relaxed scan of the S_1 potential energy surface of **6a** and found that the 180° rotation of the methoxy group involves a barrier of 0.18 eV only, a small value for an excited-state phenomenon. It is therefore likely that the "fan effect" of the methoxy group is detrimental for obtaining large quantum yields. Indeed, in general, the lone pairs of the O atom of the methoxy group are not conjugate with the pi-electrons of the dye, so that there is a fast rotation of the methyl group in OMe-substituted systems, which increase the efficiency of non-radiative deactivation. This contrasts with dialkylamino groups, in which the lone pair is generally fully conjugated with the pi-electrons (and the $NAlk_2$ group planar). By using the computed vibrationally-resolved spectra, one can determine theoretical radiative rates using a formalism detailed in the SI. For **2b**, **2c**, **4b**, **4'b**, and **6b** *ab initio* calculations return 2.77, 1.44, 3.69, 3.01, and 4.87 10^8 s^{-1}. This can be compared to the experimental values of 2.14, 1.25, 3.84, 2.14, and 3.29 10^8 s^{-1}. Obviously, both the orders of magnitude and the most significant trends in the series are reasonably reproduced by the calculations.

Let us now turn towards protonation effects that have been experimentally investigated in ethanol, a protic solvent for which the selected solvent continuum model is less efficient, so that we describe below the trends as obtained by TD-DFT rather than compare absolute values. First, one has to establish what happens upon protonation. For **2a**, **2c**, **4a**, and **6a**, there is only one protonation site available, the pyridyl. However, in all other compounds, one can envisage the protonation on either the pyridyl, the amino donor, or both groups. In **2b**, the difference between the (ground-state) Gibbs free energy of the two putative mono-protonated structures, 8.5 kcal.mol^{-1}, clearly indicates that the initial protonation takes place at the pyridyl, which follows chemical intuition. When comparing the vertical absorption of this mono-protonated form to the original **2b** (in EtOH), TD-DFT predicts a +67 nm bathochromic shift, well in line with the experimental value (+53 nm, see Table 1). The oscillator strength also increases by ca. 20%, consistent with the observed hyperchromic shift (Figure 1). In contrast, the mono protonation of the **2b** on the amino group would deliver a joint hypsochromic/hypochromic (-12 nm/-50%) evolution according to the simulations, clearly not fitting the experimental trends. Finally, the protonation of both centres is predicted to induce a small bathochromic displacement (+22 nm) but a very strong intensity decrease (-72%), which is clearly inconsistent with the measurements. In short, the theoretical calculations indicate that in acidic environment, single protonation of the carboline core takes place. To qualitatively understand this impact of protonation, Figure 5 provides the EDD of **2b** and **2b.H**$^{+}$ in EtOH. The former strongly resembles the one of Figure 4, though one can note a slightly stronger ICT character due to the increased in polarity, the ICT distance being 2.32 Å in ethanol as compared to 2.24 Å in benzene. The protonation leads to the creation of a strong accepting unit (pyridinium) and the ICT is obviously greatly enhanced. According to Le Bahers' model, 0.70 e are now transferred over 3.25 Å, typical of strong ICT transitions.

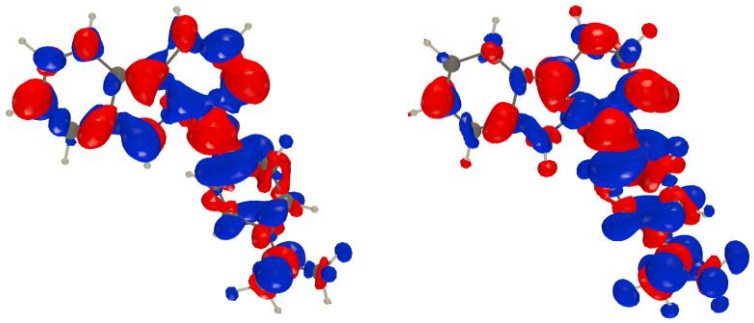

2b **2b.H$^+$**

Figure 5: EDD plot for the absorption of dyes **2b** and **2b.H$^+$** in ethanol. See caption of Fig. 4 for more details.

In Table S1 in the SI, we report the computed absorption and emission wavelengths in both neutral and acidic ethanol for all compounds. As can be seen, protonation is systematically predicted to yield a bathochromic displacement, in line with the experimental trends. In both theory and experiment, the largest shifts are obtained for **4b** and **4'b**, as the linker obviously favours strong ICT.

Conclusion

To conclude, we synthetized and studied the photophysical properties of six different β-carboline dyes substituted in the 1 position. The introduction of a strong mesomeric donor leads to a strong ICT emissive system, the emission being clearly issued from an emissive ICT state, but for compounds **2a** and **4a** that show emissive feature typical of a local excited state in benzene. All dyes are sensitive to protonation, which unambiguously takes place on the pyridine and brings a notorious bathochromic shift of both absorption and emission bands. The TD-DFT calculations provide data in good agreement with the experimental observation and confirm the proposed photophysical mechanism happening in these systems. The large redshifts between the neutral and protonated form of these structures make them interesting starting blocks for developping new fluorochromic pH sensors. Works are in progress to tune the pKa of the pyridine and to enhance the water solubility in order to obtain useable biological pH probes.

Acknowledgments

T. V. P. is indebted to M. H. E. Bousquet (Nantes University) for her fruitful help with the vibronic calculations. The authors thank the ANR for financial support in the framework of the BiBiFlu project. We acknowledge the CNRS providing research facilities and financial support and the University of Strasbourg for a MENRT fellowship for C. MARET. The authors thank the CCIPL/Glicid mesocenter installed in Nantes for generous allocation of computational time.

General procedure for synthesis of compounds 2.

Tryptophan (408 mg, 2.01 mmol) was suspended in DCM (5 mL), trifluoroacetic acid (0.5 mL) was added and the solution became limpid. Benzaldehyde (2 eq) was added and the mixture was stirred at room temperature for 1.5 hours. The solvent was removed by rotary evaporation, a saturated aqueous solution of sodium bicarbonate was then added. The mixture was filtered and washed several times with water, and was further dried with vacuum pump. After all water has been evaporated, the white solid was dissolved in anhydrous DMF (15 mL) and triethylamine (0.6 mL, 4.82 mmol). A solution of N-chlorosuccinimide (402 mg, 3.01 mmol) in DMF (15 mL) was added dropwise to the solution and stirred 2 hours. After completion, water (50 mL) was added and the mixture was extracted with AcOEt (5 X). The combined organic extract was washed several times with a saturated aqueous solution of sodium carbonate and was dried over magnesium sulfate. The solvent was removed by rotary evaporation and the residue was purified by column chromatography on silica gel to give **2a**-**2b**.

1-(4-methoxyphenyl)-9H-pyrido[3,4-b]indole (2a) yield: 221 mg (40 %) yellow powder **^{1}H NMR** (500 MHz, $CDCl_3$): δ = 8.58 (bs, 1 H), 8.54 (d, ^{3}J = 5.3 Hz, 1H), 8.16 (dd, ^{3}J = 7.8 Hz, ^{4}J = 1.0 Hz, 1H), 7.97 – 7.85 (m, 3H), 7.62 – 7.45 (m, 2H), 7.32 (ddd, ^{3}J = 7.8 Hz, ^{3}J = 6.8 Hz, ^{4}J = 1.0 Hz, 1H), 7.12 (d, ^{3}J = 8.7 Hz, 2H), 3.91 (s, 3H).

1-(4-dimethylaminophenyl)-9H-pyrido[3,4-b]indole (2b) yield: 83 mg (15 %) red powder **^{1}H NMR** (400 MHz, $CDCl_3$): δ = 8.60 – 8.48 (m, 2H), 8.15 (d, ^{3}J = 8.0 Hz, 1H), 7.93 – 7.83 (m, 3H), 7.58 – 7.47 (m, 2H), 7.30 (ddd, ^{3}J = 8.0 Hz, ^{3}J = 6.7 Hz, ^{4}J = 1.1 Hz, 1H), 6.91 (d, ^{3}J = 8.8 Hz, 2H), 3.06 (s, 6H). **^{13}C NMR** (126 MHz, $CDCl_3$): δ = 150.9, 140.5, 133.2, 129.7, 129.3, 129.1, 128.4, 122.5, 121.9, 121.7, 120.1, 112.7, 112.6, 112.5, 111.4, 40.4. **HRMS (ESI-TOF)** $C_{19}H_{17}N_3$ found: 288.1503 $[M+H]^+$, calculated: 288.1495.

General procedure for synthesis of compounds 4.

To a solution of **3** (100 mg, 0.55 mmol) or harmine **3'** (100 mg, 0.47 mmol) and benzaldehyde (3 eq) in toluene was added piperidine (1 mL) and catalytic amount of *p*-TsOH.H_2O (1 to 5 mg). The flask was equipped with a Dean-Stark apparatus and was then heated to 140 °C overnight in the dark. After cooling the reaction was treated with a saturated aqueous solution of sodium carbonate and extracted

with DCM (3x). The organic layer was washed with a saturated aqueous solution of sodium bicarbonate then brine and the solvent was removed by rotary evaporation. The residue was dissolved in EtOH, acidified with a 37% aqueous solution of HCl, evaporated, and then dissolved in 0.5 M HCl solution and wash with DCM until DCM wash became colorless. The aqueous solution is then basified with a saturated aqueous solution of sodium carbonate and extracted three times with DCM. The combined DCM extracts were then evaporated with addition of ethanol. The product was then purified by the suitable numbers of recristalisation from DCM/cyclohexane to give **4a – 4b**.

(E)-1-(4-methoxystyryl)-9H-pyrido[3,4-b]indole (4a) yield: 140 mg (84 %) yellow powder **^{1}H NMR** (400 MHz, $CDCl_3$): δ = 8.61 (s, 1H), 8.51 (d, ^{3}J = 5.2 Hz, 1H), 8.16 (d, ^{3}J = 7.9 Hz, 1H), 7.91 – 7.81 (m, 2H), 7.65 – 7.55 (m, 4H), 7.43 (d, ^{3}J = 15.9 Hz, 1H), 7.34 (ddd, ^{3}J = 7.9 Hz, ^{3}J = 5.8 Hz, ^{4}J = 1.2, 1H), 6.95 (d, ^{3}J = 8.8 Hz, 2H), 3.87 (s, 3H).

(E)-1-(4-dimethylaminostyryl)-9H-pyrido[3,4-b]indole (4b) yield: 39 mg (22 %) red powder **^{1}H NMR** (400 MHz, $CDCl_3$): δ = 8.91 (bs, 1H), 8.48 (d, ^{3}J = 5.2 Hz, 1H), 8.13 (d, ^{3}J = 7.8 Hz, 1H), 7.86 – 7.80 (m, 2H including d, ^{3}J = 15.2 Hz), 7.60 – 7.43 (m, 2H), 7.45 (d, ^{3}J = 8.4 Hz, 2H), 7.37 – 7.28 (m, 2H including d, ^{3}J = 16 Hz), 6.67 (d, ^{3}J = 8.4 Hz, 2H), 2.99 (s, 6H). **^{13}C NMR** (101 MHz, $CDCl_3$): δ = 150.6, 140.9, 140.2, 139.4, 133.7, 133.6, 129.5, 128.4, 128.3, 124.9, 122.1, 121.8, 120.2, 118.3, 112.8, 112.2, 111.6, 40.3. **HRMS (ESI-TOF)** $C_{21}H_{19}N_3$ found: 314.1645 $[M+H]^+$, calculated : 314.1652.

(E)-1-(4-dimethylaminostyryl)-7-methoxy-9H-pyrido[3,4-b]indole (4'b) yield: 142 mg (88 %) red powder **^{1}H NMR** (500 MHz, $CDCl_3$): δ = 8.66 (s, 1H), 8.43 (d, ^{3}J = 5.2 Hz, 1H), 7.97 (d, ^{3}J = 8.6 Hz, 1H), 7.77 (d, ^{3}J = 15.8 Hz, 1H), 7.70 (d, ^{3}J = 5.2 Hz, 1H), 7.49 (d, ^{3}J = 8.8 Hz, 2H), 7.29 (d, ^{3}J = 15.8 Hz, 1H), 7.01 (d, ^{4}J = 2.1 Hz, 1H), 6.91 (dd, ^{3}J = 8.6 Hz, ^{4}J = 2.1 Hz, 1H), 6.68 (d, ^{3}J = 8.8 Hz, 2H), 3.92 (s, 3H), 2.99 (s, 6H). **^{13}C NMR** (126 MHz, $CDCl_3$): δ = 160.9, 150.6, 141.8, 140.2, 139.6, 133.6, 133.4, 129.7, 128.3, 125.0, 122.6, 118.4, 115.9, 112.2, 112.1, 109.6, 94.9, 58.5, 40.3. **HRMS (ESI-TOF)** $C_{22}H_{21}N_3O$ found: 344.1744 $[M+H]^+$, calculated: 344.1757.

General procedure for synthesis of compound 6.

The bromine derivative **5** (40 mg, 0.16 mmol), ethynyl (3 eq) and $Pd(dppf)Cl_2$ (12 mg, 0.02 mmol) in THF/Et_3N (5/0.5 mL) were placed in a Schlenk tube. The solution was degassed with argon for 15 min, and CuI (5 mg, 0.02 mmol) was then added. The mixture was stirred at room temperature overnight. The residue was washed with a saturated aqueous solution of sodium carbonate and extracted with DCM (3x). The organic layer was dried over magnesium sulfate and the solvent was removed by rotary evaporation. The product was purified twice by column chromatography on silica gel (AcOEt/DCM/EP/Et_3N, 10:30:60:1) then (AcOEt/toluene/PE/Et_3N 20:50:30:1) to give **6a - 6b**.

1-((4-methoxyphenyl)ethynyl)-9H-pyrido[3,4-b]indole (6a) yield: 46 mg (99 %) yellow powder **^{1}H NMR** (400 MHz, $CDCl_3$): δ = 8.73 (bs, 1H), 8.49 (d, ^3J = 5.2 Hz, 1H), 8.13 (d, ^3J = 7.9 Hz, 1H), 7.91 (d, ^3J = 5.2 Hz, 1H), 7.65 – 7.54 (m, 4H), 7.38- 7.28 (m, 1H), 6.90 (d, ^3J = 7.0 Hz, 2H), 3.84 (s, 3H). **^{13}C NMR** (126 MHz, $CDCl_3$): δ = 160.2, 140.2, 139.8, 133.6, 129.1, 128.8, 128.3, 127.3, 125.3, 122.0, 121.9, 120.4, 114.4, 114.1, 111.8, 94.5, 84.1, 55.4. **HRMS (ESI-TOF)** $C_{20}H_{14}N_2O$ found: 299.1165 $[M+H]^+$, calculated : 299.1179.

1-((4-dimethylaminophenyl)ethynyl)-9H-pyrido[3,4-b]indole (6a) yield: 40 mg (80 %) yellow powder **^{1}H NMR** (500 MHz, $CDCl_3$): δ = 8.59 (bs, 1H), 8.47 (d, ^3J = 5.2 Hz, 1H), 8.13 (dd, ^3J = 7.9 Hz, ^4J = 0.9 Hz, 1H), 7.88 (dd, ^3J = 5.2 Hz, ^5J = 0.7 Hz, 1H), 7.61 – 7.52 (m, 4H), 7.33 - 7.29 (m, 1H), 6.69 (d, ^3J = 9.0 Hz, 2H), 3.03 (s, 6H). **^{13}C NMR** (126 MHz, $CDCl_3$): δ = 150.65, 139.97, 139.91, 136.98, 133.30, 128.66, 128.54, 127.96, 122.02, 120.40, 113.92, 111.77, 111.69, 108.63, 96.19, 83.51, 40.18. **HRMS (ESI-TOF)** $C_{21}H_{17}N_3$ found: 312.1484 $[M+H]^+$, calculated: 312.1495.

References:

[1] P. F. Rosales, G. S. Bordin, A. E. Gower, S. Moura, *Fitoterapia* **2020**, *143*, 104558.

[2] D. Singh, S. Sharma, M. Kumar, I. Kaur, R. Shankar, S. K. Pandey, V. Singh, *Organic & Biomolecular Chemistry* **2019**, *17*, 835–844.

[3] J. Hamill, J. Hallak, S. M. Dursun, G. Baker, *Curr.Neuropharmacol.* **2019**, *17*, 108–128.

[4] M. Moloudizargari, P. Mikaili, S. Aghajanshakeri, M. Asghari, J. Shayegh, *Phcog Rev* **2013**, *7*, 199.

[5] M. Sater, D. Stephens, *Biochem Soc Trans* **1989**, *17*, 81.

[6] M. Silva F. C. Savar, *J Brazil chem soc* **2016**, *27*, 1558

[7] T. Herraiz, C. Chaparro, *Journal of Chromatography A* **2006**, *1120*, 237

[8] R. Cao, W. Peng, Z. Wang, A. Xu, *Current Medicinal Chemistry* **2007,** *14*, 479

[9] M. Curran, G. Keating, *Drugs* **2003**, *63*, 2203

[10] S. A. Bouwman, R. Zoleko-Manego, K. C. Renner, E. K. Schmitt, G. Mombo-Ngoma, M. P. Grobusch, *Travel Medicine and Infectious Disease* **2020**, *36*, 101765.

[11] T. Duka, B. Schutt, W. Krause, R. Dorow, S. McDonald, K. Fichte, *British Journal of Clinical Pharmacology* **1993**, *35*, 386–394.

[12] S. J. Stachel, S. A. Stockwell, D. L. Van Vranken, *Chemistry and Biology* **1999**, *6*, 531

[13] R. Duval, C. Duplais *Nat. Prod. Rep* **2017**, *34*, 161

[14] Z. Cao, Y. Yu, P. Hao, Z. Di, Y. He, Z; Chen, W. Yang, Z. Shen, X. He, J. Sheng, X. Xu, B. Pan, J. Feng, X. Yang, W. Hong, W. Zhao, Z. Li, K. Huang, T. Li, Y. Kong, H. Liu, D. Jiang, B. Zhang, J. Hu, Y. Hu, B. Wang, J. Dai, B. yuan, Y. Feng, W. Haung, X. Xing, G. Zhao, X. Li, Y, Li, W. Li *Nat. Commun* **2013**, *4*, 2602

[15] O. S. Wolfbeis, E. Fürlinger, *Zeitschrift für Physikalische Chemie* **1982**, *129*, 171–183.

[16] A. Sánchez-Coronilla, M. Balón, M. A. Muñoz, J. Hidalgo, C. Carmona, *Chemical Physics* **2008**, *351*, 27–32.

[17] A. Sánchez Coronilla, C. Carmona, M. A. Muñoz, M. Balón, *J Fluoresc* **2010**, *20*, 163–170.

[18] Y.-F. Sun, Z.-Y. Chen, Y.-L. Liu, N. Li, J.-K. Li, H.-C. Song, *Dyes and Pigments* **2012**, *95*, 512–522.

[19] K. Imato, T. Enoki, Y. Ooyama, *RSC Adv.* **2019**, *9*, 31466–31473.

[20] S. Swami, D. Behera, A. Agarwala, V. P. Verma, R. Shrivastava, *New J. Chem.* **2018**, *42*, 10317–10326.

[21] S. A. Mousa, P. Douglas, H. D. Burrows, S. M. Fonseca, *Photochem. Photobiol. Sci.* **2013**, *12*, 1606.

[22] V. Y. Shuvalov, V. A. Elisheva, A. S. Belousova, E. V. Arshinov, L. V. Glyzdinskaya, M. A. Vorontsova, S. A. Chernenko, A. S. Fisyuk, G. P. Sagitullina, *Chem Heterocycl Comp* **2020**, *56*, 73–83.

[23] I. X. García-Zubiri, H. D. Burrows, J. S. Seixas de Melo, M. Monteserín, A. Arroyo, M. J. Tapia, *J Fluoresc* **2008**, *18*, 961–972.

[24] F. A. O. Rasse-Suriani, F. S. García-Einschlag, M. Rafti, T. Schmidt De León, P. M. David Gara, R. Erra-Balsells, F. M. Cabrerizo, *Photochem Photobiol* **2018**, *94*, 36–51.

[25] D. Reyman, C. Díaz-Oliva, F. Hallwass, S. M. Gonçalves de Barros, *RSC Adv.* **2011**, *1*, 857.

[26] J. Dillon, A. Spector, K. Nakanishi, *Nature*, **1976**, *259*, 422-423.

[27] M. Singh, P. Awasthi, V. Singh, *EurJOC*, **2020**, *8*, 1023-1041

[28] J. Y. Pu, B. Chen, W. Wu, C. Yang, G, Zhang, J. J. Chruma, *ACS Omega*, **2021**, *18*, 12238-12249

[29] S. Sarkar, P. Pandya, K. Bhadra, *Plos One 9*, **2014**, *9*, e108022.

[30] M, Singh, Vaishali, S. Kumar, R. Jamra, S. K. Pandey, V. Singh, Tetrahedron, 2020, 47, 131640-131655

[31] A. Kamal, M. Sathish, A. V. G. Prasanthi, J. Chetna, Y. Tangella, V. Srinivasulu, N. Shankaraiah, A. Alarifi, *RSC Advances* **2015**, *5*, 90121–90126.
[32] F. Bracher, D. Hildebrand, *Tetrahedron* **1994**, *50*, 12329–12336.
[33] C. A. Guido, A. Chrayteh, G. Sclamani, B. Mennucci, D. Jacquemin *J. Chem. Theory Comput.* **2021**, *17*, 5155−5164.
[34] T. Le Bahers, C. Adamo, I. Ciofini, *J. Chem. Theory Comput.* **2011**, *7*, 2498–2506
[35] P. F. Loos, D. Jacquemin, *ChemPhotoChem.* **2019**, *3*, 684–696.
[36] J. Olmsted. *J. Phys. Chem*. **1979**, *83*, 2581–2584.